

Ablation spectra of the human cornea

David Cohen

Laser Laboratory
Cedars-Sinai Medical Center
University of California, Los Angeles
Biomedical Engineering Department
Los Angeles, California

Roy Chuck

University of California, Irvine
Department of Ophthalmology
Irvine, California

Greg Bearman

Jet Propulsion Laboratory
California Institute of Technology
Pasadena, CA

Peter McDonnell

University of California, Irvine
Irvine, California

Warren Grundfest

Laser Laboratory, Cedars-Sinai Medical Center
University of California, Los Angeles
Biomedical Engineering Department
Los Angeles, California

Laser corneal surgery systems in current clinical use rely on ultraviolet laser-induced ablation. Typically, these systems selectively remove tissue to optimize the air–cornea interface geometry, although a significant number of cases involve the removal of superficial corneal opacities resulting from disease or injury. Despite the notable success and popularity of laser corneal surgery, some variability occurs in postoperative visual acuity. It is natural to ask whether the fluorescence emitted during ablation affords the possibility of closed-loop surgical feedback that provides improved predictability of postoperative visual acuity. Laser ablation also effectively removes abnormal corneal tissue [a procedure known as phototherapeutic keratotomy (PTK)], which often is highly scattering in comparison with normal cornea and hence obstructs vision. Removal of such abnormal tissue is performed entirely at the surgeon's discretion, based in part upon the surgeon's perception of the tissue fluorescence, which alters noticeably as the ablation exposes healthy tissue. Towards these ends, this paper evaluates the relationship between the tissue fluorescence generated during ablation and the degree of ablation. The cornea is a layered structure consisting of the outermost epithelial layer, the stroma, and the endothelium adjacent to the aqueous humour (see Figure 1). Previous work has shown spectral differentiation between the epithelium and the stroma, but had not explored ablative fluorescence in greater detail.^{1–3}

When used to alter the imaging properties of the cornea, an estimate of tissue volume distribution to be removed is based

Abstract. Ablation of human corneal tissue with 193 nm excimer laser energy generates fluorescence in the near ultraviolet and visible regions of the spectrum. The fluorescence spectra from five human corneas were collected during ablation *in vitro*. We find that the fluorescence spectrum changes continuously as the cornea is ablated from the epithelial surface towards the endothelium. We reduced the dimensionality of the large data set resulting from each cornea by a principal components analysis. The three most significant principal component eigenvectors suffice to describe the observed spectral evolution, and independent analysis of each tissue sample produces a similar set of eigenvectors. The evolution of the calculated eigenvector weighting factors during ablation then corresponds to the observed spectral evolution. In fact, this evolution is qualitatively consistent between corneas. We suggest that this spectral evolution offers promise as a real-time surgical feedback tool. © 2001 Society of Photo-Optical Instrumentation Engineers. [DOI: 10.1117/1.1380670]

Keywords: cornea; fluorescence; lasers; ablation.

Paper JBO-20004 received Mar. 1, 2000; revised manuscript received Dec. 19, 2000; accepted for publication Mar. 14, 2001.

upon a preoperative measurement of both corneal topography and measured refractive error. All clinically approved corneal ablation methods, such as PRK (photorefractive keratotomy) and LASIK (laser-assisted *in situ* keratomileusis), proceed open loop (without real time feedback indicating progress of the ablation) as the system completes a precalculated ablation pattern. Clinically approved ablation methods designed to alter the focal length of the cornea are empirically derived from large clinical studies. These studies established a statistical correlation between corneal topography, visual acuity, and the tissue removal pattern predicted to optimize vision. However, these correlations were derived assuming a constant ablation rate. This method fails to account for variations in tissue that may occur with patient age^{4,5} or certain disease processes. Despite the great success that open loop ablation surgery has enjoyed, there appears to be room for improvement by introducing feedback control of the ablation. In this paper, we present studies of the fluorescence of human corneal samples *in vitro*, under conditions that reasonably approximate those in the operating room, to determine whether such fluorescence might prove useful for surgical control.

The histology of the cornea is well documented: marked differences exist between the three primary layers of the cornea: epithelium, stroma, and endothelium. The outermost layer of the cornea, the corneal epithelium, is a 50 μm multilayer of cells having rapid turnover. The epithelium rests upon Bowman's membrane, a 6–9 μm thick largely acellular layer of randomly arranged collagen fibrils. The stroma constitutes the preponderance of the cornea and is relatively sparsely populated by cells, consisting rather of a matrix of various collagens. The posterior surface of the stroma is covered by Descemet's membrane, which is intermediate between

David Cohen is currently employed by the Optical Systems Modeling Group at the Jet Propulsion Laboratory. He may be contacted at: Mail Stop 306-336, Jet Propulsion Laboratory, 4800 Oak Grove Drive, Pasadena, CA 91109-8099. Tel: 818-354-2794; Fax: 818-393-4489; E-mail: cohendx@cshs.org. Address all correspondence to Greg Bearman, ANE Image, 974 E Elizabeth, Pasadena, CA. E-mail: gbearman@jpl.nasa.gov

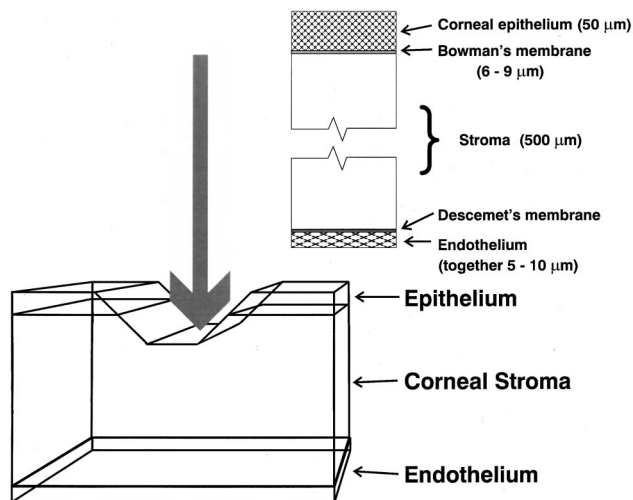


Fig. 1 A schematic cross section of the cornea, showing the three primary layers and indicating the direction of ablation. The epithelium is approximately $50\ \mu\text{m}$ thick, the endothelium $10\ \mu\text{m}$, and the stroma $500\ \mu\text{m}$.

the stroma and the endothelial layer of cells. The endothelium itself is a single layer of longer-lived cells. Together, Descemet's membrane and the endothelium are typically $6\text{--}9\ \mu\text{m}$ in thickness.

The evolution in structure of the ablative spectra described here may be consistent with numerous biochemical and structural differences known to exist between the anterior and posterior portions of the cornea and corneal stroma. The anterior lamellae of human corneas are known to be interwoven, whereas the posterior lamellae are not.⁶ This is not surprising considering the different developmental origins of these two regions. That is, the anterior one third of the stroma appears to be of different developmental origin than the posterior two thirds.⁷ In addition to collagens, other components are known to exist in the cornea. However, knowledge of concentrations and spatial distributions is sparse. It has also been shown, in bovine corneas, that the concentration and types of glycosaminoglycans varies with corneal depth.^{8,9} The ratio of keratin sulfate proteoglycan to dermatan sulfate proteoglycan is greater in the posterior than the anterior stroma. In fact, the cloudiness seen in macular corneal dystrophy is thought to be related to failure of synthesis of mature keratin sulfate proteoglycans.¹⁰ The transparency of the cornea results from local constructive interference, minimizing scatter. Destructive interference is greatest in the posterior and least in the anterior stroma for rabbits and humans,¹¹ suggesting depth-dependent structural variations. It is reasonable to postulate that specific compositional details vary with age as well as the presence of corneal disease. The fluorescence of cells as well as collagens is discussed in detail in the literature.

We used human corneas rejected for transplantation because of pseudoepithelium, sepsis, or extended storage time. The corneas were acquired from a local eye bank from donors showing no signs of corneal disease or systemic disease known to affect the cornea. The tissue as supplied included both the clear cornea and the limbus. Tissue was supplied in standard ophthalmic transplant solution, which was thoroughly rinsed from the samples with distilled water or physi-

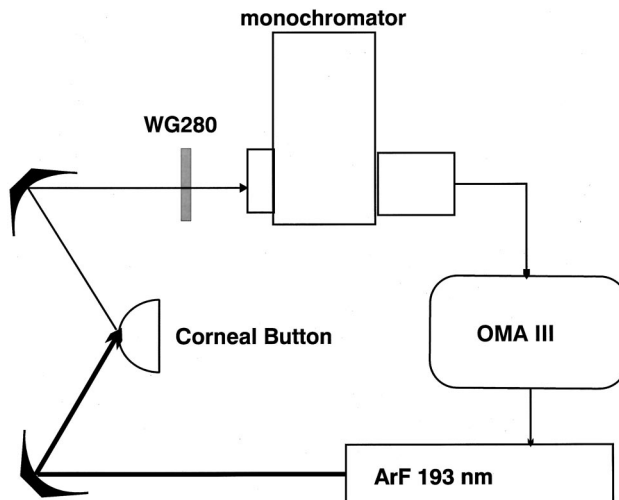


Fig. 2 Optical layout used in this paper.

ologic saline before use in fluorescence experiments. The contribution of the fluorescence spectrum from any remaining components of the preservative solution is shown to be both small and independent of ablation depth. In order to eliminate potential fluorescence from the corneal mounting jig, the entire sample was mounted using a nonfluorescent arrangement of stainless steel hypodermic needles either piercing or supporting the opaque limbus. The tissue was thus suspended in free space, with the optic axis near the focus of the ablating laser beam. Because $193\ \text{nm}$ photons excite fluorescence from most materials, it was not practical to attempt to isolate the fluorescence spectrum of the preservative solution alone.

We implemented the laser-induced corneal ablation system using a $193\ \text{nm}$ Questek ArF excimer laser. The experimental layout appears in Figure 2. An aluminum mirror focused the excimer laser beam onto the epithelial side of the corneal sample. This method minimizes fluorescence from optics in the laser beam path. In order to maintain the fluence at the corneal surface at clinical values, we placed the sample a few millimeters before the geometrical point of focus. This produced a rectangular laser spot approximately $4.5\ \text{mm}$ by $3\ \text{mm}$ in size in the sample plane (this compares with a $1\text{--}6.5\ \text{mm}$ spot size typical of commercial corneal ablation systems). Fluence on the corneas was approximately $170\ \text{mJ}/\text{cm}^2$, near clinical levels. To collect the fluorescence emitted during ablation, we placed an aluminum off-axis paraboloid to image the ablated region onto the entrance slit of a $0.3\ \text{m}$ monochromator. The relatively high degree of optical aberration associated with off-axis paraboloids precluded any attempt at distinguishing between fluorescence from the tissue and that of the ablation plume. A coarse $150\ \text{groove}/\text{mm}$ grating mounted in the monochromator permitted simultaneous acquisition of the entire spectral range ($200\text{--}900\ \text{nm}$) with a linear focal plane array detector. A lumogen-coated ultraviolet sensitive silicon diode array (EG&G Reticon) captured the light dispersed by the grating. By placing a $3\ \text{mm}$ thick Schott W280 long wavelength pass filter before the entrance slit and as far from the cornea as possible we minimized collection of the secondary fluorescence excited within the filter glass by energetic $193\ \text{nm}$ photons.

An EG&G OMA III triggered both the excimer laser and Reticon array readout. The excimer laser operated at a pulse repetition rate slightly less than 1 Hz, producing a nominal 1 ns long pulse. We programmed the OMA to acquire and store each emission spectrum generated by a series of 65 consecutive laser shots, repeating this procedure until physical perforation of the tissue sample occurred. In principle, we could have stored each of the thousands of spectra generated by the series of laser shots necessary to achieve tissue perforation. However, we found that the emission spectra change quite slowly as the corneal stroma ablates so that storage of every group of spectra from the stroma was unnecessary.

The data resulting from the experiment consisted of multiple arrays of spectra, each array corresponding to a different ablation depth. Changes in the spectra were not evident from one laser shot to the next, but were readily apparent upon comparison of spectra separated by a significant number of laser shots. Therefore, we chose to average all 65 spectra within each acquisition sequence to reduce the overall size of the data set to the number of acquisition sequences. The averaging of 65 shots removed any chance of observing effects from ablating through Bowman's membrane as it is $\sim 6\text{--}9\ \mu\text{m}$ thick. Note that the spectra are not corrected for wavelength dependent system throughput, as our goal is simply to observe changes in the system under test. When so corrected, these spectra agree with those determined in earlier work.^{1,2} The data were smoothed in the spectral domain by a 25-pixel moving average. The temporal and spectral averaging employed in this initial report effectively limits the resolution of the method. We estimate the spectral resolution at 30 nm, which is consistent with the smoothing applied. In fact, the spectral features central to this report are much broader than our resolution. Averaging of 65 single-shot ablation spectra reduces the depth sensitivity of the present analysis. Assuming the ablation depth increment generated by a single laser pulse at clinical fluence levels to be $0.25\ \mu\text{m}$, we can estimate our depth sensitivity to on the order of 65 times that depth, $16.3\ \mu\text{m}$. This estimate of ablation rate is consistent with the number of shots necessary to ablate our corneas to perforation.

The analysis algorithm chosen is one commonly used to investigate variations in a multivariate data set. In this case multivariate refers to the simultaneous measurement at multiple wavelengths of spectral energy density, i.e., photoablation spectra. These measurements were made repeatedly under varying conditions—progressively increasing ablation depth. As a preprocessing step every individual photoablation spectrum was normalized to its own area, and the mean fluorescence spectrum of each cornea was subtracted from each individual spectrum measured from that cornea.

We applied principal components analysis (PCA) to the normalized data. This algorithm attempts to describe each high-dimensional measurement vector (spectrum) to a low-dimensional descriptive vector.¹² In this report, we summarize a spectrum measured at several hundred wavelengths using a three dimensional vector. Independently tracking the variation in the first, second, and third component of these vectors as ablation progresses, we find distinct patterns described later in this paper.

Stated another way, PCA provides a set of orthonormal eigenvectors spanning the linear space defined by all of the

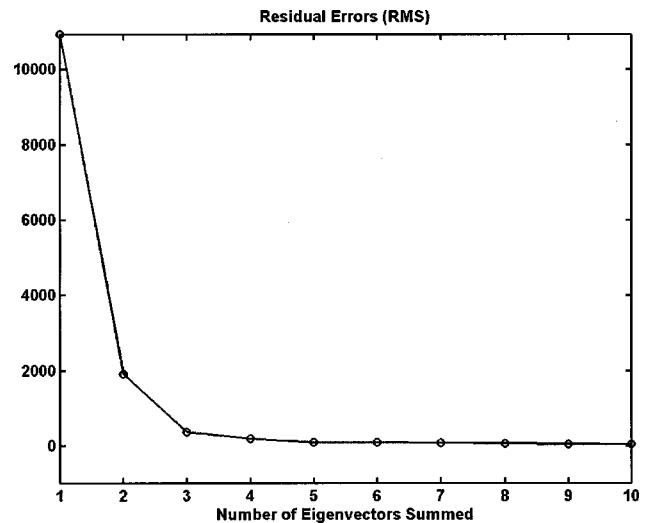


Fig. 3 The principal components analysis discussed in the text utilizes the first three eigenvalues to approximate the measured spectra. In order to demonstrate the fidelity of this approximation, the mean rms error is shown for the first (epithelial) spectrum of all five corneas. The error appears as a function of the number of eigenvectors summed.

acquired spectra from a corneal sample; any spectrum from that data set can be then approximated in the least squares sense as a linear combination of these eigenvectors. The analysis also generates the coefficients of the linear combination used to produce a particular spectrum also result from the singular value decomposition. Mathematically, the analysis is implemented as a singular value decomposition (SVD) of the data matrix X , where each normalized spectrum is one row of X . SVD approximates X in the least squares sense by the product of three matrices UDV' where U and V are orthonormal. Matrix U contains weighting coefficients, while matrix V contains the eigenvectors. The remaining matrix D is diagonal and contains the eigenvalues. Typically in principal components analysis, each eigenvector is multiplied by the corresponding diagonal element of D . Here we choose to work with the normalized eigenvectors and consider the eigenvalues separately. This technique permits compact graphical presentation of spectral features on a common scale. Figure 3 indicates the relative errors incurred in an approximation to an epithelial spectrum that uses between one and ten eigenvectors to build the approximation.

In Figure 4, we plot a summary of the spectral evolution measured during the ablation of the five normal corneas. We performed an independent principal components analysis on the spectral data from each cornea. Each row in the figure corresponds to a different cornea. In the first column, each figure depicts the first three most significant eigenvectors as a function of wavelength. Because the weightings (D) are not included, each coefficient can be plotted on the same vertical scale. Note that the sharp peak at longer wavelengths with some corneas corresponds to leakage of scattered laser light appearing in third order. The coefficients of each eigenvector as a function of shot group number appears in the second column of plots. The data show that some corneas required more laser shots to achieve perforation. This follows from the variation in angle of incidence inherent in mounting flexible

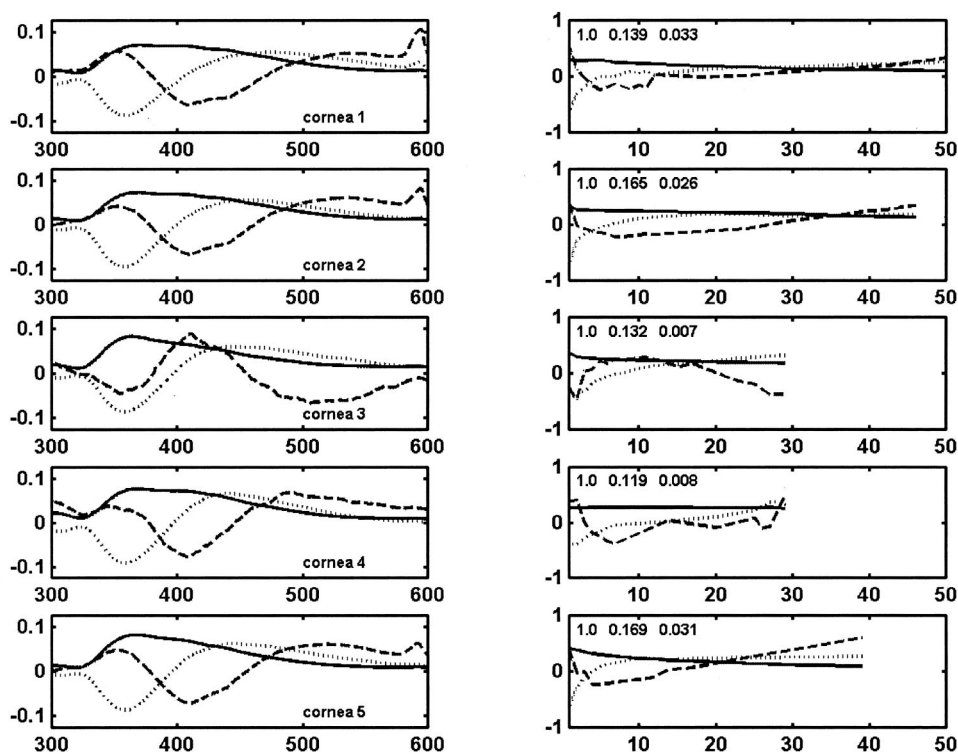


Fig. 4 The plots summarize the results for the five corneas studied, with each row corresponding to a different cornea. The left hand column presents the eigenvectors calculated from the full set of fluorescence spectra collected from the relevant cornea, while the right hand column shows the evolution of the eigenvector weighting with shot number. The first three eigenvalues from the singular value decomposition appear in the upper left hand corner of the weighting plots, normalized so that the first eigenvalue is always unity. The weighting factor represented by a solid line decreases monotonically, while that represented by small dashes increases monotonically. The third weighting factor initially decreases, then increases.

tissue with minimum support—increasingly off-normal incidence increases the thickness of the cornea as viewed along the laser beam path. We found no significant changes in ablation rate that could be attributed to the slightly shorter pulse width of the Questek laser.

The fourth cornea is anomalous, a fact we attribute to the especially long delay between harvest and measurement for this sample (i.e., tissue degradation). In the other four corneas, we find a similar set of eigenvectors, suggesting a set of easily accessible spectral features. Furthermore, the coefficients evolve in a characteristic manner. The most rapid changes occur within the first few shots, in which the thin corneal epithelium is rapidly ablated. The spectral evolution then slows markedly as the stroma is exposed. This slower evolution validates our use of lower sampling density relative to shot number in this regime.

The spectral evolution presented here cannot be unequivocally attributed to chemical gradients within the cornea without further work. Nevertheless, the behavior observed during corneal ablation offers considerable promise as a quantitative clinical feedback parameter in ultraviolet (UV) laser induced corneal ablation. Clinical experience correlates visual observation of fluorescence with ablation progress during PRK or LASIK-type procedures. The behavior that we observe *in vitro* most likely reflects known composition gradients along the epithelium–endothelium axis. We must consider some alternative hypotheses, however. The simplest relates to chang-

ing hydration of the tissue during the experiment. Because of the low repetition rate of the laser, some time is necessary to ablate to perforation. While we found that corneal hydration was partially maintained during the experiment by suspension of a water droplet from the sample, we also tested the effects of hydration on the spectrum. No significant change was observed in the emission spectrum when a free-standing cornea was wetted with water. It is also possible that ablation causes photochemical changes. Such changes are limited to the close vicinity of each ablated volume because of the rapid spatial attenuation of the excimer photons and most fluorescence. Unfortunately, the relevance of photochemistry to the spectral evolution is difficult to test. Furthermore, a photochemically induced modification of the fluorescence spectrum does not by any means detract from the usefulness of the fluorescence spectrum as a feedback parameter.

Finally, we note that the laser spot on the cornea was not perfectly sharp edged (see Figure 5). Therefore, ablation at the extreme periphery proceeded more slowly than at the center, and the fluorescent spectrum acquired at each shot reflects an admixture of signals emanating from various depths below the corneal epithelium. In other words, the depth resolution of the experiment was limited by the transverse gradients in the excimer laser beam at the ablation plane. For these reasons we see little reason to seek higher spectral or depth resolution in data from this experimental configuration.

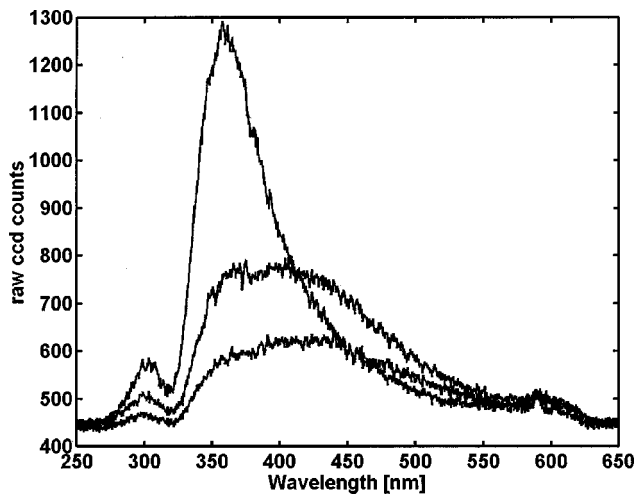


Fig. 5 Plots of three raw single shot photoablation spectra at various depths taken during the experimental run on one cornea used in this study. These spectra are unsmoothed and unnormalized. Note that the spectral features are quite broad. The spectrum in the highest peak was recorded while the ablation was just beginning in the corneal epithelium. The peak intensity drops essentially monotonically as ablation proceeds deeper into the cornea.

We have shown that the broadband fluorescence generated during *in vivo* ablation of human corneal tissue evolves with increasing ablation depth in a consistent manner when tissue decomposition is not too excessive. This fluorescence data offer promise as a useful tool when results are correlated with corneal disease and postablation healing. Our data were measured under conditions similar to clinical parameters, with

the exception of a low repetition rate used to simplify data collection.

References

1. A. F. Phillips and P. J. McDonnell, "Laser-induced fluorescence during photorefractive keratectomy: A method for controlling epithelial removal," *Am. J. Ophthalmol.* **123**, 42–47 (1997).
2. S. Tuft, R. Al-Dharir, P. Dyer, and Z. Zehao, "Characterization of the fluorescence spectra produced by excimer laser irradiation of the cornea," *Invest. Ophthalmol. Visual Sci.* **31**, 1512–1518 (1990).
3. L. Uma, Y. Sharma, and Balasubramanian, "Fluorescence properties of isolated intact normal human corneas," *Photochem. Photobiol.* **63**, 213–216 (1996).
4. P. S. Hersh, O. D. Schein, and R. Steinert, "Characteristics influencing outcomes of excimer laser photorefractive keratectomy. Summit photorefractive keratectomy phase III study group," *Ophthalmology* **103**, 1962–1969 (1996).
5. T. Papaioannou, E. Maguen, A. B. Nesburn, J. J. Salz, J. I. Macy, J. Hofbauer, and W. Grundfest, "The effect of age on the refractive outcome of myopic photorefractive keratectomy with the VISX 20/20 laser," *Invest. Ophthalmol. Visual Sci.* **39**, S349 (1998).
6. F. M. Polak, "Morphology of the cornea: I: Study with silver stains," *Am. J. Ophthalmol.* **51**, 179–184 (1961).
7. J. W. McTigue, "The human cornea: A light and electron microscopic study of the normal cornea and its alterations in various dystrophies," *Trans. Am. Ophthalmol. Soc.* **65**, 591–660 (1967).
8. R. Bettelheim and B. Plessy, "The hydration of proteoglycans of bovine cornea," *Biochim. Biophys. Acta* **381**, 203–214 (1975).
9. J. Castoro, A. Bettelheim, and F. Bettelheim, "Water gradients across bovine cornea," *Invest. Ophthalmol. Visual Sci.* **29**, 963–968 (1988).
10. J. R. Hassell, D. A. Newsome, J. H. Drachmer, and M. M. Rodrigues, "Macular corneal dystrophy: Failure to synthesize a mature keratan sulfate proteoglycan," *Proc. Natl. Acad. Sci. U.S.A.* **77**, 3705–3709 (1980).
11. D. E. Freund, R. L. McCally, R. A. Farrell, S. M. Cristol, N. L. L'Hernault, and H. F. Edelhauser, "Ultrastructure in anterior and posterior stroma of perfused human and rabbit corneas," *Invest. Ophthalmol. Visual Sci.* **36**, 1508–1523 (1995).
12. P. Geladi and H. Grahn, *Multivariate Image Analysis*, Wiley, New York (1996).